JPE 16-4-5

http://dx.doi.org/10.6113/JPE.2016.16.4.1288
ISSN(Print): 1598-2092 / ISSN(Online): 2093-4718

A Single-Stage LED Tube Lamp Driver with Input-Current Shaping for Energy-Efficient Indoor Lighting Applications

Chun-An Cheng*, Chien-Hsuan Chang*, Hung-Liang Cheng*, Tsung-Yuan Chung*, Ching-Hsien Tseng*, and Kuo-Ching Tseng†

*Department of Electrical Engineering, I-Shou University, Kaohsiung City, Taiwan
†Department of Electronic Engineering, National Kaohsiung First University of Science and Technology, Kaohsiung City, Taiwan

Abstract

This study proposes a single-stage light-emitting diode (LED) tube lamp driver with input-current shaping for T8/T10-type fluorescent lamp replacements. The proposed AC–DC LED driver integrates a dual-boost converter with coupled inductors and a half-bridge series-resonant converter with a bridge rectifier into a single-stage power conversion topology. This paper presents the operational principles and design considerations for one T8-type 18 W-rated LED tube lamp with line input voltages ranging from 100 V rms to 120 V rms. Experimental results for the prototype driver show that the highest power factor (PF = 0.988), lowest input current total harmonic distortion (THD = 7.22%), and highest circuit efficiency (η = 92.42%) are obtained at an input voltage of 120 V. Hence, the proposed driver is feasible for use in energy-efficient indoor lighting applications.

Key words: Converter, Driver, Light-emitting diode (LED)

I. INTRODUCTION

Fluorescent lamps are cost-effective gas-discharge lamps for general indoor lighting applications. As a result of the current issues in environmental protection, carbon reduction and energy savings have become a cause for great concern, and the search for energy-efficient alternatives for lighting applications has intensified at a global scale. The up-to-date development of solid-state lighting technology has gained traction because of the urgent need for efficient energy usage [1]-[5]. Light-emitting diodes (LEDs) are compact electronic devices that allow electricity to flow through them in one direction to produce a small amount of light. Tube lamps and bulbs for household usage include a large number of LEDs; thus, these fixtures produce bright light. LEDs offer numerous attractive features, such as their non-polluting property because of the absence of mercury as a component, high luminous efficacy, long lifetime, and significant energy savings brought about by their low power consumption [6]-[17]. Therefore, LEDs are beginning to replace traditional lighting sources used in households and other indoor lighting applications. As an illustrated example, Table I shows a comparison between a T8-type fluorescent lamp (China Electric FL40D-EX) and a T8-type LED tube lamp (EVERLIGHT FBW/T8/857/U/4ft) [18], [19]. The two lamps share almost the same color temperature and color-rendering index, but the LED tube lamp achieves better lighting efficiency, consumes less power, and offers longer lamp lifetime than its T8-type counterpart. Moreover, the LED tube lamp contains no mercury and does not require high ignition voltage. Therefore, energy-efficient LED tube lamps have become increasingly popular alternatives to fluorescent lamps for use in household and other indoor lighting applications, such as in public infrastructure, offices, classrooms, and parking decks [20]-[25]. Fig. 1 shows a typical two-stage driver for a T8-type LED tube lamp. This driver is composed of an AC–DC converter with power factor corrections (PFC)

Manuscript received Nov. 26, 2015; accepted Feb. 21, 2016
Recommended for publication by Associate Editor Yan Xing.
†Corresponding Author: jerry@nkfust.edu.tw
Tel: +886-7-6011000 ext.2516, National Kaohsiung First University of Science and Technology
*Dept. of Electrical Eng., I-Shou University, Taiwan

TABLE I
COMPARISON BETWEEN T8-TYPE FLUORESCENT AND LED TUBE LAMPS

Items	T8-type Fluorescent Lamp (China Electric FL20D-EX/18)	T8-type LED Tube Lamp (EVERLIGHT FBW/T8/857/U/4ft)
Consumed Power	20 W	18 W
Lumen Output	1,440 lm	1,800 lm
Lamp Current	0.35 A	0.3 A
Lighting Efficiency	> 88 lm/W	> 100 lm/W
Color Temperature	6,700 K	5,700 K
Color Rendering Index R_a	> 80	> 80
Lamp Life	> 7,500 h	> 35,000 h
Lamp Base	G13	G13
Mercury Content	Yes	No
Requirement for High Ignition Voltage	Yes (> 400 V)	No

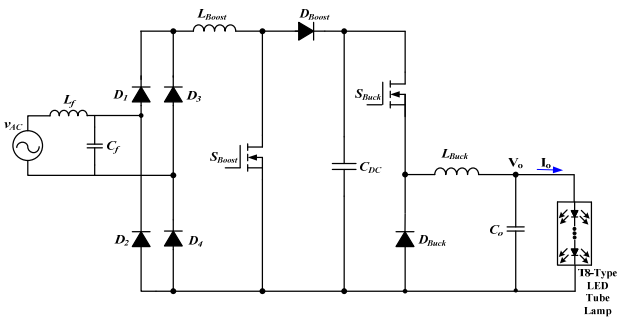

Fig. 1. Typical two-stage driver for a T8-type LED tube lamp.

as the first stage (such as a boost converter) and a DC–DC converter (such as a buck converter) as the second stage for regulating the voltage/current of the LED lamp. The converter in each stage requires a separate control scheme, and the circuit efficiency is restricted because of the two-stage power conversion. A number of single-stage AC–DC drivers for T8-type LED tube lamps, which are used as alternatives to T8/T10 fluorescent lamps, have been introduced, with flyback converters, buck converters, and buck-boost converters serving as the main circuit topology of the drivers in [23], [24], and [25] and all featuring PFC. These single-stage versions offer cost-effectiveness and low component counts in comparison with their two-stage counterparts; however, their power switches do not include a soft-switching function, hence their limited efficiencies.

In response to these concerns, the present study proposes a single-stage AC–DC driver with input-current shaping and enhanced circuit efficiency for use in a T8-type LED tube lamp. Moreover, this study presents the theoretical analysis of the operating modes and the experimental results obtained from the prototype circuit of the proposed driver used to supply an 18 W-rated T8-type LED tube lamp. The paper is organized as follows. Section II describes and analyzes the proposed LED tube lamp driver. Section III presents the design considerations of the proposed LED tube lamp driver. Section IV describes the experimental results obtained from a prototype LED driver for an 18 W-rated T8-type LED tube lamp with input utility line voltages ranging from 100 V to 120 V. Finally, Section V provides relevant conclusions.

II. DESCRIPTION AND ANALYSIS OF THE PROPOSED LED TUBE LAMP DRIVER

Fig. 2 shows the proposed LED tube lamp driver, which combines a dual-boost converter with coupled inductors. Specifically, one boost converter contains a diode D_{b1}, a coupled inductor L_{PFC1}, a switch S_1, the body diode of switch S_2, and a DC-linked capacitor C_{DC}; the other boost converter includes a diode D_{b2}, a coupled inductor L_{PFC2}, a switch S_2, the body diode of switch S_1, and a capacitor C_{DC}. The figure also shows a half-bridge series-resonant converter with a bridge rectifier; it includes a DC-linked capacitor C_{DC}, two switches S_1 and S_2, a resonant inductor L_r, a resonant capacitor C_r, a full-bridge rectifier D_1–D_4, and an output capacitor C_o. These components are combined into a single-stage topology for a T8-type LED tube lamp. In addition, an LC filter (inductor L_f and capacitor C_f) is connected to the input utility line voltage [26].

To analyze the operations of the proposed driver for an LED lamp, the following assumptions are made.

(a) The switching frequencies of switches S_1 and S_2 are significantly higher than that of the utility line voltage v_{AC}. Hence, the sinusoidal utility line voltage can be considered as a constant value for each high-frequency switching period.
(b) Power switches are complementarily operated, and their inherent diodes are considered.
(c) The analysis is simplified with the exclusion of the LC filter in the analysis of the operation modes of the driver circuit.
(d) The conducting voltage drops of diodes D_{b1}, D_{b2}, D_1, D_2, D_3, and D_4 are neglected.
(e) Two coupled inductors (L_{PFC1} and L_{PFC2}) are designed to be operated in discontinuous conduction mode to naturally achieve PFC.

The operating modes and theoretical waveforms of the proposed LED tube lamp driver operated during the positive half cycle of the input utility line voltage are shown in Figs. 3 and 4, respectively. The operations are analyzed in detail in the following sections.

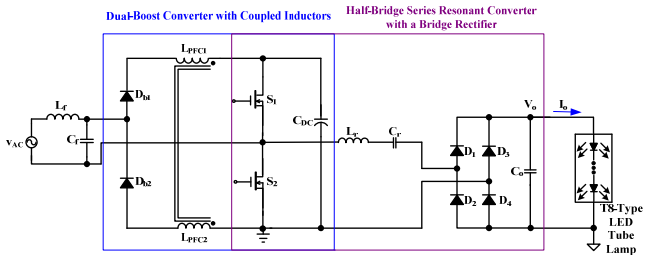

Fig. 2. Proposed single-stage driver for a LED tube lamp.

Mode 1 ($t_0 \le t < t_1$; in Fig. 3(a)): This mode begins when the voltage v_{DS1} of S_1 decreases to zero. Thereafter, the body diode of switch S_1 is forward-biased at time t_0. The resonant capacitor C_r provides energy to the resonant inductor L_r, capacitors C_{DC} and C_o, and LED tube lamp through the body diodes D_2 and D_3 of S_1. This mode ends when S_1 shifts to the on state with zero-voltage switching (ZVS) at time t_1.

Mode 2 ($t_1 \le t < t_2$; in Fig. 3(b)): This mode begins when S_1 achieves ZVS turn-on at t_1. The input voltage v_{AC} provides energy to the coupled inductor L_{PFC1} through the diode D_{b1} and switch S_1. The inductor current i_{LPFC1} linearly increases from zero and can be expressed as

$$i_{LPFC1}(t) = \frac{\sqrt{2}v_{AC-rms}\sin(2\pi f_{AC}t)}{L_{PFC1}}(t - t_1), \quad (1)$$

where $v_{AC\text{-}rms}$ is the root-mean-square (rms) value of the input utility line voltage and f_{AC} is the utility line frequency.

The resonant capacitor C_r still provides energy to the resonant inductor L_r, capacitors C_{DC} and C_o, and LED tube lamp through the switch S_1 and diodes D_2 and D_3. This mode finishes when the current i_{Lr} decreases to zero at t_2.

Mode 3 ($t_2 \le t < t_3$; in Fig. 3(c)): The voltage v_{AC} still provides energy to the coupled inductor L_{PFC1} through the diode D_{b1} and switch S_1. The DC bus capacitor C_{DC} supplies energy to the inductor L_r, capacitors C_r and C_o, and LED tube lamp through the switch S_1 and diodes D_1 and D_4. At t_3, the switch S_1 shifts to the off state, and the inductor current reaches its peak value; this condition is defined as $i_{LPFC1\text{-}pk}(t)$, which is given by

$$i_{LPFC1-pk}(t) = \frac{\sqrt{2}v_{AC-rms}\sin(2\pi f_{AC}t)}{L_{PFC1}}DT_S, \quad (2)$$

where D and T_S are the duty cycle and switching period of the power switch, respectively.

Mode 4 ($t_3 \le t < t_4$; in Fig. 3(d)): This mode starts when the power switch S_1 is in the off state at t_3. The utility line voltage v_{AC} and coupled inductor L_{PFC1} supply energy to the drain-source capacitor of S_1 through the diode D_{b1}. The inductor current i_{LPFC1} linearly decreases from the peak level and can be given by

$$i_{LPFC1}(t) = \frac{\sqrt{2}v_{AC-rms}\sin(2\pi f_{AC}t) - V_{DC}}{L_{PFC1}}(t - t_3), \quad (3)$$

where V_{DC} is the voltage of the DC-bus capacitor C_{DC}.

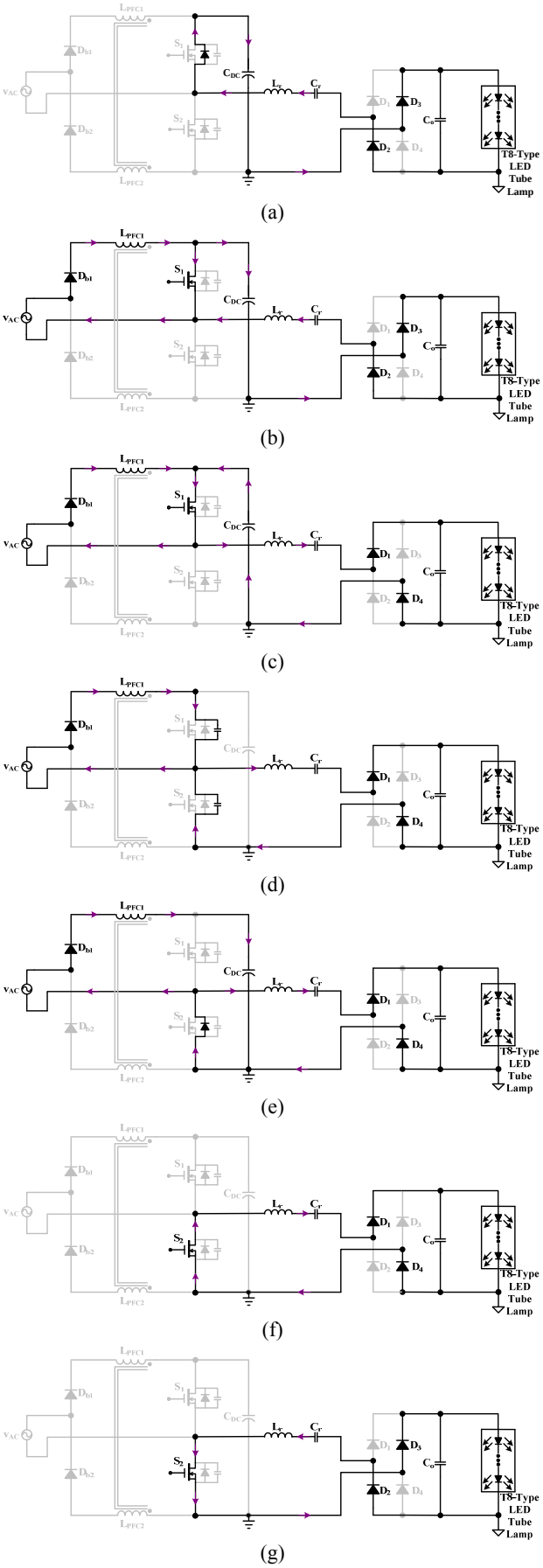

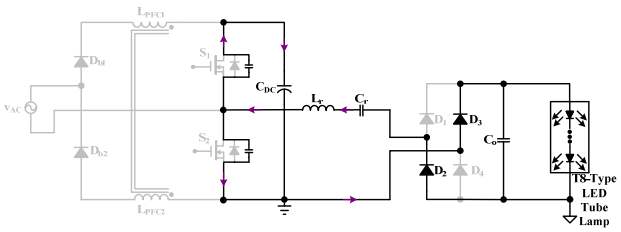

(h)

Fig. 3. Operation modes of the proposed driver during the positive half cycle of input voltage v_{AC}.

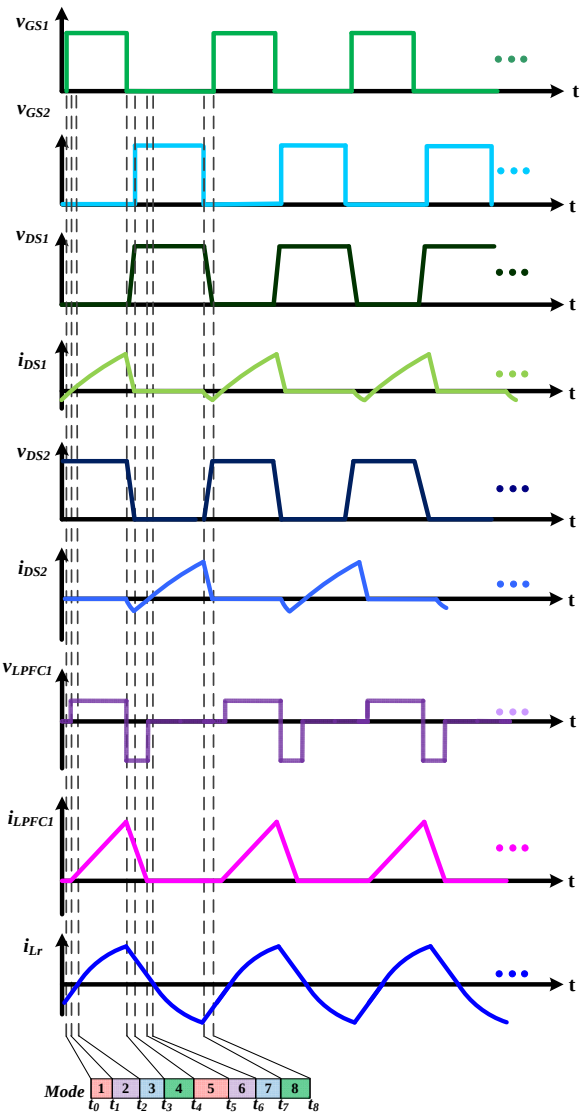

Fig. 4. Theoretical waveforms during the positive half cycle of input voltage v_{AC}.

The drain-source capacitor of S_2 provides energy to the inductor L_r, capacitors C_r and C_o, and LED tube lamp through the diodes D_1 and D_4. This mode ends when the drain-source voltage v_{DS2} of S_2 decreases to zero at t_4.

Mode 5 ($t_4 \le t < t_5$; in Fig. 3(e)): This mode starts when the voltage v_{DS2} of S_2 decreases to zero and the body diode of switch S_2 is forward-biased at time t_4. The utility line voltage

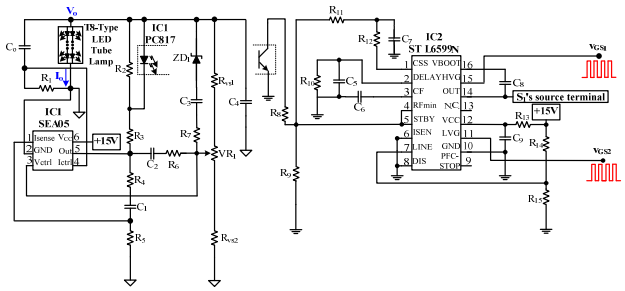

Fig. 5. Control circuit for the proposed LED tube lamp driver.

v_{AC} and coupled inductor L_{PFC1} provide energy to C_{DC} through the diode D_{b1} and body diode of switch S_2. The inductor L_r provides energy to the capacitors C_r and C_o and LED tube lamp through the diodes D_1 and D_4. At t_5, the inductor current i_{Lr} decreases to zero, and the mode ends.

Mode 6 ($t_5 \le t < t_6$; in Fig. 3(f)): This mode begins when the switch S_2 achieves ZVS turn-on at t_5. The resonant inductor L_r provides energy to the capacitors C_r and C_o and LED tube lamp through S_2 and the diodes D_1 and D_4. At t_6, the inductor current i_{Lr} decreases to zero, and the mode ends.

Mode 7 ($t_6 \le t < t_7$; in Fig. 3(g)): During this mode, the capacitor C_r provides energy to the inductor L_r, capacitor C_o, and LED tube lamp through S_2 and the diodes D_2 and D_3. The mode ends when the switch S_2 shifts to the off state at t_7.

Mode 8 ($t_7 \le t < t_8$; in Fig. 3(h)): During this mode, the resonant capacitor C_r and drain-source capacitor of switch S_1 provide energy to the DC-linked capacitor C_{DC}, drain-source capacitor of S_2, capacitor C_o, and LED tube lamp through the diodes D_2 and D_3. This mode ends when the drain-source voltage v_{DS1} of S_1 decreases to zero at t_8. Then, *Mode 1* begins for the next high-frequency switching period.

Fig. 5 shows the circuit diagram for controlling the single-stage LED tube lamp driver. Utilizing a constant voltage/current controller (IC1 SEA05) to regulate the output voltage and current of the LED lamp, we determine the output lamp voltage V_o through the resistors R_{vs1}, VR_1, and R_{vs2}, as well as the output lamp current through the resistor R_1. The sensed output signal from pin 5 of the IC1 is fed into the high-voltage resonant controller (IC3 ST L6599) through a photo-coupler (IC2 PC817). Two gate-driving signals v_{GS1} and v_{GS2} are generated from pins 15 and 11 of the IC3, respectively, to regulate the output voltage and current of the LED tube lamp.

III. Design Considerations for Key Components of the Proposed LED Driver

A. *Design of Coupled Inductors L_{PFC1} and L_{PFC2}*

The design equation for the coupled inductor L_{PFC1} (L_{PFC2}) is expressed as [26]

$$L_{PFC1} = \frac{\eta v_{AC-rms}^{\ 2} D^2}{2P_{lamp} f_S} = L_{PFC2} \quad , \tag{4}$$

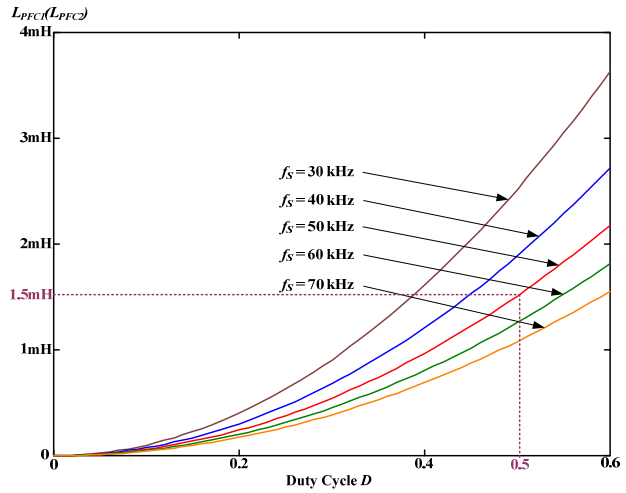

Fig. 6. Coupled inductors L_{PFC1} and L_{PFC2} versus duty cycle D under different switching frequencies f_S.

where η is the estimated circuit efficiency, P_{lamp} is the rated power of the LED lamp, and f_S is the switching frequency.

Fig. 6 shows the coupled inductors L_{PFC1} and L_{PFC2} versus the duty cycle D under different switching frequencies. With η of 0.9, $v_{AC\text{-}rms}$ of 110 V and P_{lamp} of 18 W, f_S of 50 kHz, and D of 0.5, the coupled inductors L_{PFC1} and L_{PFC2} are designed to be 1.5 mH.

B. Design of Series Resonant Tank (Lr and Cr)

Fig. 7 depicts the equivalent circuit for designing the series resonant tank; R_o is the equivalent resistance of the T8-type LED tube lamp and can be written as $R_o = V_o/I_o$. As shown in Fig. 7, the series resonant tank is composed of a resonant inductor L_r in a series connection with a resonant capacitor C_r. The resonant frequency f_o can be expressed as

$$f_o = \frac{1}{2\pi\sqrt{L_r C_r}}. \tag{5}$$

The design considerations for the series resonant tank L_r and C_r are shown in the following.

(a) The estimated efficiency η_R of the bridge rectifier component is expressed as [27]

$$\eta_R = \frac{1}{1+\frac{2V_F}{V_o}+\frac{\pi^2 R_F}{4R_o}+\frac{r_C}{R_o}\left(\frac{\pi^2}{8}-1\right)}, \tag{6}$$

where V_F and R_F are the forward voltage drop and equivalent resistor of the diodes, respectively, and r_C is the equivalent resistor of capacitor C_o.

With r_C of 50 mΩ, R_o of 200 Ω, V_F of 1.5 V, and R_F of 0.15 Ω (according to the datasheet of the utilized diode), the estimated efficiency η_R is given by

$$\eta_R = \frac{1}{1+\frac{2\cdot 1.5}{60}+\frac{\pi^2\cdot 0.15}{4\cdot 200}+\frac{0.05}{200}\left(\frac{\pi^2}{8}-1\right)} = 0.95.$$

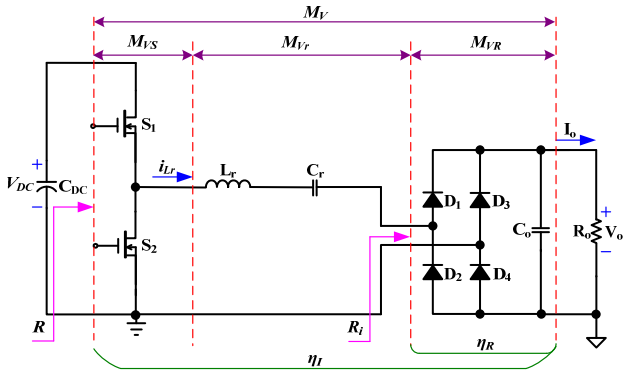

Fig. 7. Equivalent circuit for designing the series resonant tank.

(b) The input resistor R_i of the bridge rectifier is expressed as

$$R_i = \frac{8R_o}{\pi^2\eta_R} = \frac{8\cdot 200}{\pi^2\cdot 0.95} = 170.6\Omega. \tag{7}$$

(c) The voltage gain M_{VR} of the bridge rectifier is expressed as

$$M_{VR} = \frac{\pi\eta_R}{2\sqrt{2}} = \frac{\pi\cdot 0.95}{2\sqrt{2}} \cong 1.1. \tag{8}$$

(d) The total voltage gain M_V of the half-bridge series resonant converter with a bridge rectifier is expressed as

$$M_V = \frac{V_o}{V_{DC}} \cong \frac{V_o}{2\sqrt{2}\cdot v_{AC-\max}} = \frac{60}{2\sqrt{2}\cdot 120} \cong 0.17. \tag{9}$$

(e) The voltage gain M_{Vr} of the series resonant component is expressed as

$$M_{Vr} = \frac{M_V}{M_{VS}M_{VR}}, \tag{10}$$

where M_{VS} is the voltage gain of the half-bridge converter. With M_{VS} of 0.45 (=√2/π), the voltage gain M_{Vr} is given as

$$M_{Vr} = \frac{0.17}{0.45\cdot 1.1} \cong 0.3.$$

(f) The loaded quality factor Q_L is expressed as [27]

$$Q_L = \frac{\sqrt{\frac{\eta_I^2}{M_{Vr}^2}-1}}{\left|\frac{f_s}{f_o}-\frac{f_o}{f_s}\right|}, \tag{11}$$

where η_I is the estimated efficiency of the half-bridge series resonant converter with a bridge rectifier.

To obtain the ZVS for the two active switches, the switching frequency f_S is designed to be larger than the resonant frequency f_o so that the resonant tank resembles an inductive network [27].

Therefore, the relationship between switching frequency f_S and resonant frequency f_0 is assumed as

$$f_s = 4f_o. \tag{12}$$

With η_I of 0.99 and f_s of 50 kHz, the quality factor Q_L is given as

$$Q_L = \frac{\sqrt{\frac{0.99^2}{0.3^2}-1}}{\left|4-\frac{1}{4}\right|} = 0.84 .$$

(g) The input resistor R of the half-bridge series resonant converter with a bridge rectifier is expressed as

$$R = \frac{R_i}{\eta_I} = \frac{170.6}{0.99} = 172.3\Omega . \quad (13)$$

(h) The resonant capacitor C_r is expressed as and computed with

$$C_r = \frac{1}{2\pi f_o Q_L R} = \frac{1}{2\pi \cdot 50k/4 \cdot 0.84 \cdot 172.3} = 87.9\mu F . \quad (14)$$

In addition, C_r is set to 82 nF.

(i) The resonant inductor L_r is expressed as and computed with

$$L_r = \frac{1}{(2\pi f_o)^2 C_r} = \frac{1}{\left(2\pi \cdot 50k/4\right)^2 \cdot 82n} = 1.98mH . \quad (15)$$

In addition, L_r is set to 2 mH.

IV. Experimental Results for a Prototype Driver

A prototype driver was built and tested for an 18 W-rated T8-type LED tube lamp (EVERLIGHT FBW/T8/857/U/4ft), the rated voltage and current of which are 60 V and 0.3 A, respectively. The components utilized in the LED tube lamp driver are shown in Table II.

Fig. 8 shows the measured inductor currents i_{LPFC1} and i_{LPFC2}. The measured switch voltage v_{DS2} and inductor current i_{Lr} are depicted in Fig. 9. The series resonant tank resembles an inductive load. Figs. 10 and 11 present the measured voltages (v_{DS1} and v_{DS2}) and currents (i_{DS1} and i_{DS2}) of the two power switches S_1 and S_2, respectively. ZVS is obviously achieved for these power switches, consequently boosting the circuit efficiency.

Fig. 12 shows the measured output voltage and current waveforms; the average values of V_o and I_o are 60 V and 0.3 A, respectively. Table III presents the measured output voltage and current of the proposed LED tube lamp driver under different input voltages. In addition, the output voltage (current) ripple is obtained with the peak-to-peak (pk-pk) level divided by the average value of the output voltage (current). According to this table, the highest and lowest measured output voltage ripples are 7.29% and 5.93%, respectively; these ripples occurred at utility line rms voltages of 100 and 120 V, respectively. Moreover, the highest and lowest measured output current ripples are 9.5% and 8.48%, respectively; these ripples occurred at utility line rms voltages of 120 and 105 V, respectively. The measured input utility

TABLE II
Key Components Used in the Proposed LED Tube Lamp Driver

Component	Value
Filter Inductor (L_f)	3.3 mH
Filter Capacitor (C_f)	0.47 μF/250 V
Power Switches (S_1, S_2)	IRF840
Coupled Inductors (L_{PFC1}, L_{PFC2})	1.5 mH
DC-linked Capacitor (C_{DC})	220 μF/450 V
Resonant Inductor (L_r)	2 mH
Resonant Capacitor (C_r)	82 nF
Diodes (D_{b1}, D_{b2})	MUR460
Diodes (D_1, D_2, D_3, D_4)	C3D10060
Output Capacitor (C_o)	470 μF/63 V ×2

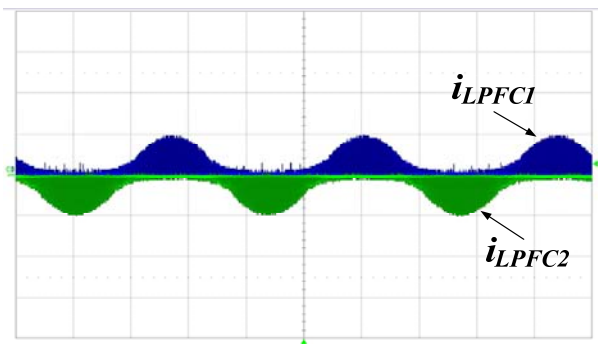

Fig. 8. Measured inductor currents i_{LPFC1} (1 A/div) and i_{LPFC2} (1 A/div); time scale: 5 ms/div.

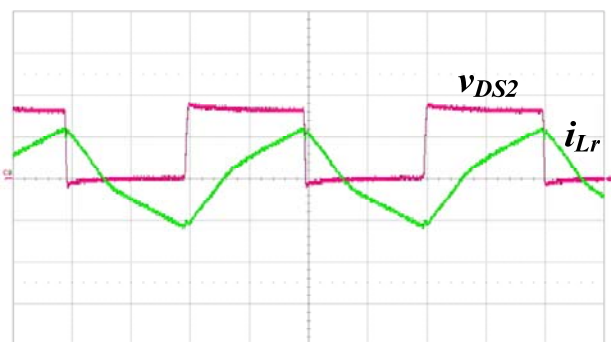

Fig. 9. Measured voltage v_{DS2} (200 V/div) and inductor current i_{Lr} (0.5 A/div); time scale: 5 μs/div.

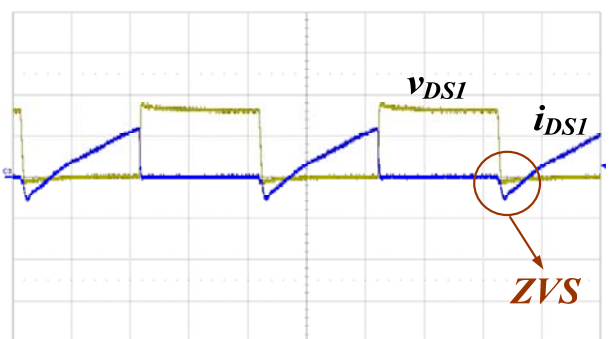

Fig. 10. Measured voltage v_{DS1} (200 V/div) and current i_{DS1} (0.5 A/div); time scale: 5 μs/div.

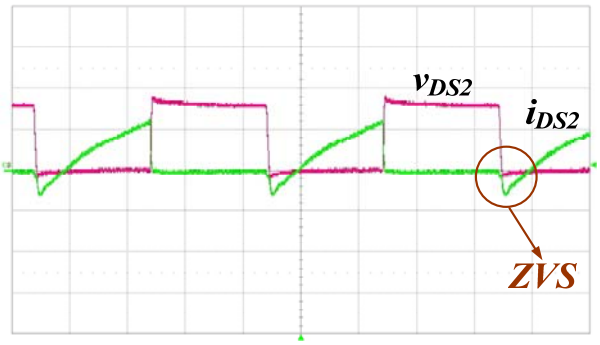

Fig. 11. Measured voltage v_{DS2} (200 V/div) and current i_{DS2} (0.5 A/div); time scale: 5 μs/div.

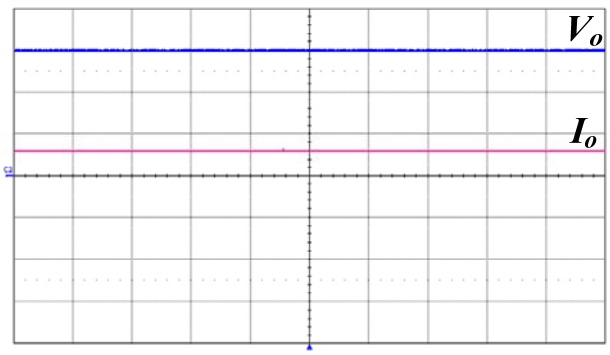

Fig. 12. Measured output voltage V_o (20 V/div) and current I_o (0.5 A/div); time scale: 2 ms/div.

TABLE III
MEASURED OUTPUT VOLTAGE AND CURRENT OF THE PRESENTED LED TUBE LAMP DRIVER UNDER DIFFERENT INPUT VOLTAGES

Input Voltage / Parameters	100 V	105 V	110 V	115 V	120 V
Output Voltage (mean)	60.22 V	60.19 V	60.07 V	60.17 V	60.23 V
Output Voltage (pk-pk)	4.39 V	4.1 V	4.14 V	3.98 V	3.57 V
Output Voltage Ripple Ratio	7.29 %	6.81 %	6.89 %	6.61 %	5.93 %
Output Current (mean)	303.8 mA	304.1 mA	300.1 mA	303.8 mA	303.7 mA
Output Current (pk-pk)	26.04 mA	25.8 mA	27.06 mA	28.12 mA	28.85 mA
Output Current Ripple Ratio	8.57 %	8.48 %	9.02 %	9.26 %	9.5 %

line voltage and current are shown in Fig. 13. Fig. 14 presents the measured current harmonics compared with the IEC 61000-3-2 Class C standards under input utility line voltages ranging from 100 V to 120 V. All the measured current

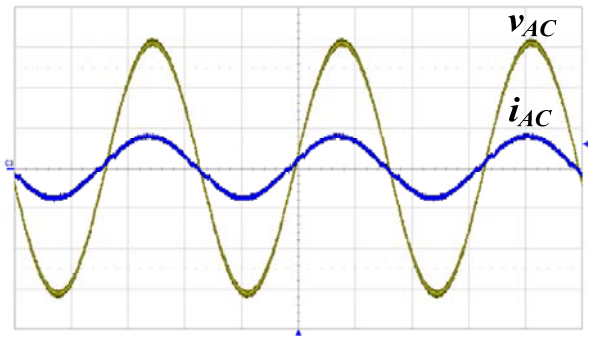

Fig. 13. Measured input utility line voltage v_{AC} (50 V/div) and current i_{AC} (0.5 A/div); time scale: 5 ms/div.

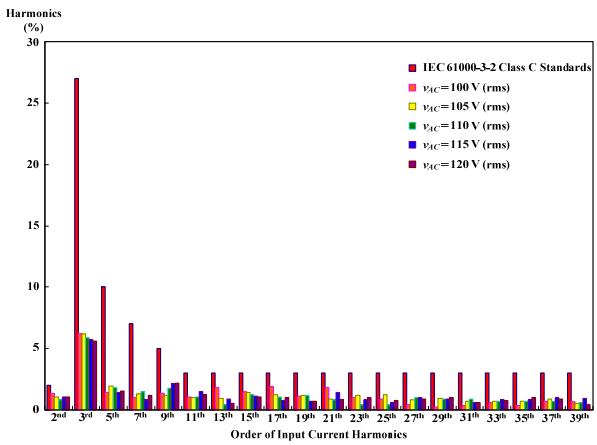

Fig. 14. Measured input current harmonics compared with the IEC 61000-3-2 Class C standards.

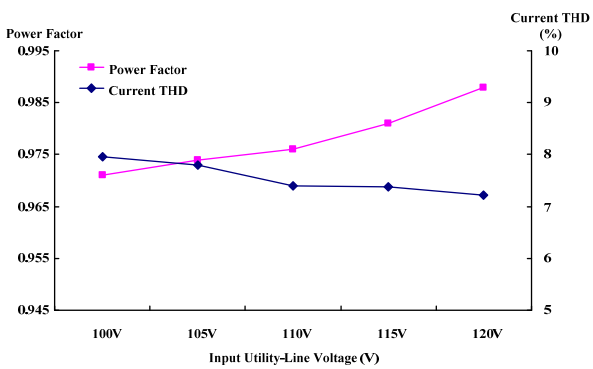

Fig. 15. Measured PF and current THD of the proposed LED driver under different input utility line voltages.

harmonics meet the requirements. Fig. 15 shows the measured power factor (PF) and current total harmonic distortion (THD) at input utility line voltages ranging from 100 V to 120 V. At a utility line rms voltage of 110 V, the measured PF and current THD are 0.976 and 7.39%, respectively. Fig. 16 shows the measured efficiency of the proposed LED tube lamp driver under input utility line voltages from 100 V to 120 V. The highest and lowest measured efficiency levels are 92.42% and 90.98% at utility line rms voltages of 120 and 100 V, respectively.

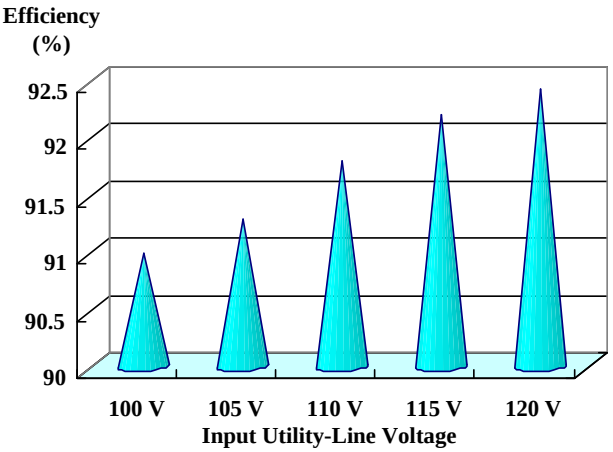

Fig. 16. Measured efficiency under different input utility line voltages.

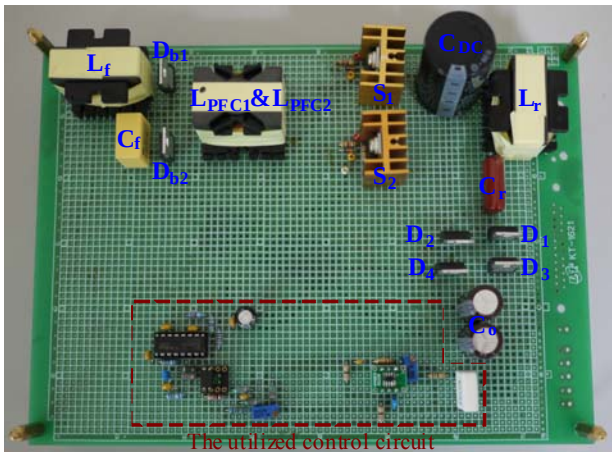

Fig. 17. Designed prototype of the proposed LED tube lamp driver.

TABLE IV
COMPARISON OF EXISTING SINGLE-STAGE T8-TYPE LED TUBE LAMP DRIVERS AND THE PROPOSED DRIVER

Item	Existing Driver #1 [23]	Existing Driver #2 [24]	Existing Driver #3 [25]	Proposed Driver
Circuit Topology	Flyback Converter	Buck Converter	Buck-boost Converter	Integration of a dual-boost converter with a half-bridge series converter
Input Utility Line Voltages	90–264 V AC	90–264 V AC	85–135 V AC	10–120 V AC
Output Rated Power	19 W (42 V/0.45 A)	18.3 W (39 V/0.47 A)	20 W (85 V/0.235 A)	18 W (60 V/0.3 A)
Measured Maximum Power Factor	0.99 @ 110 V	0.96 @ 110 V	0.996 @ 115 V	0.988 @ 120 V
Measured Minimum Current THD	9% @ 180 V	21.54% @ 110 V	4.1% @ 115 V	7.22% @ 120 V
Measured Maximum Efficiency	87.8% @ 180 V	88.56% @ 180 V	87.6% @ 135 V	92.42% @ 120 V

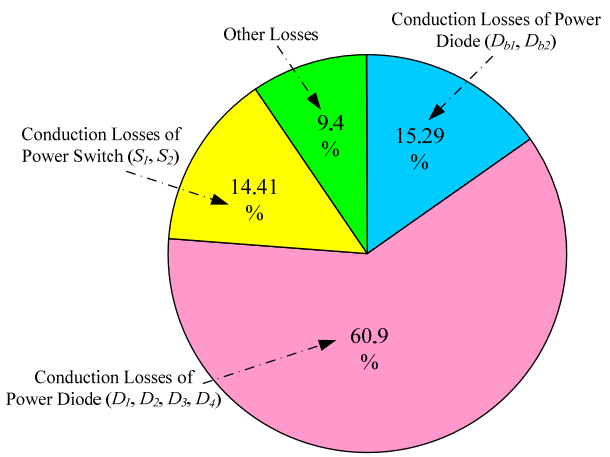

Fig. 18. Loss breakdown chart of the proposed LED tube lamp driver.

Table IV shows a comparison of the performance (including maximum PF, minimum current THD, and maximum efficiency) of the proposed driver and various LED tube lamp drivers. The first driver [23] features a flyback converter circuit topology, the second driver [24] features a buck converter circuit topology, and the third driver [25] features a buck-boost converter circuit topology. Two of the AC–DC LED drivers ([23] and [24]) operate with universal input voltages, whereas the other driver [25] and the proposed version operate with American utility line voltages. Table IV shows that the proposed single-stage LED tube lamp driver achieves ZVS on the power switches to enhance circuit efficiency in contrast to the three single-stage drivers.

Fig. 17 shows a picture of the designed prototype of the proposed LED tube lamp driver. Fig. 18 presents the loss breakdown chart of the proposed LED tube lamp driver. The percentages of the conduction losses of the power switches (S_1, S_2), power diodes (D_{b1}, D_{b2}), and power diodes (D_1, D_2, D_3, D_4), as well as the other losses are 14.41%, 15.29%, 60.9%, and 9.4%, respectively. The dominant losses in the

proposed driver with a soft-switching feature comprise the conduction losses of the power devices (including the power switches and power diodes), the percentages of which reach 90.6% of the total losses.

V. CONCLUSIONS

This study proposed a single-stage LED tube lamp driver with PFC. This driver integrates a dual-boost converter with coupled inductors and a half-bridge series resonant converter with a bridge rectifier for energy-efficient indoor lighting applications. A prototype circuit was successfully built for an 18 W-rated T8-type LED tube lamp with utility line voltages ranging from 100 V to 120 V. The experimental results revealed high PF (>0.97), low THD (<8%), and high efficiency (>90%), which verify the functionality of the proposed LED driver.

REFERENCES

[1] V. C. Bender, T. B. Marchesan, and J. M. Alonso, "Solid-state lighting: A concise review of the state of the art on LED and OLED modeling," *IEEE Ind. Electron. Mag.*, Vol. 9, No. 2, pp. 6-16, Jun. 2015.

[2] P. S. Almeida, D. Camponogara, H. Braga, M. Dalla-Costa, and J. M. Alonso, "Matching LED and driver life spans: A review of different techniques," *IEEE Ind. Electron. Mag.*, Vol. 9, No. 2, pp. 36-47, Jun. 2015.

[3] "LED lighting solutions," ON Semiconductor, http://www.onsemi.cn/pub_link/Collateral/BRD8034-D.PDF, pp. 1-48, Mar. 2013.

[4] "High brightness LED driver solutions for general lighting," ON Semiconductor, http://www.onsemi.cn/pub_link/Collateral/TND345-D.PDF

[5] B. Johnson and J. Lee, "Solutions for today's low-power LED lighting trends," *Fairchild Semiconductor*, pp. 1-11, 2011.

[6] E. F. Schubert, *Light-emitting diodes*, Cambridge University Press, 2006.

[7] D. Camponogara, G. F. Ferreira, A. Campos, M. Dalla-Costa, and J. Garcia, "Offline LED driver for street lighting with an optimized cascade structure," *IEEE Trans. Ind. Appl.*, Vol. 49, No. 6, pp. 2437–2443, Nov./Dec. 2013.

[8] P. S. Almeida, A. L. C. Mello, H. A. C. Braga, M. A. Dalla Costa, and J. M. Alonso, "Off-line soft-switched LED driver based on an integrated bridgeless boost-half-bridge converter," in *IEEE Industry Applications Society Annual Meeting*, pp. 1-7, Oct. 2013.

[9] T. J. Liang, W. J. Tseng, J. F. Chen, and J. P. Wu, "A novel line frequency multistage conduction LED driver with high power factor," *IEEE Trans. Power Electron.*, Vol. 30, No. 9, pp. 5103-5115, Sep. 2015.

[10] C. S. Moo, Y. J. Chen, and W. C. Yang, "An efficient driver for dimmable LED lighting," *IEEE Trans. Power Electron.*, Vol. 27, No. 11, pp. 4613-4618, Nov. 2012.

[11] R. L. Lin, Y. C. Chang, and C. C. Lee, "Optimal design of LED array for single-loop CCM buck-boost LED driver," *IEEE Trans. Ind. Appl.*, Vol. 49, No. 2, pp. 761–768, Mar./Apr. 2013.

[12] C. Y. Wu, T. F. Wu, J. R. Tsai, Y. M. Chen, and C. C. Chen, "Multistring LED backlight driving system for LCD panels with color sequential display and area control," *IEEE Trans. Ind. Electron.*, Vol. 55, No. 10, pp. 3791-3800, Oct. 2008.

[13] Y. L. Lin, H. J. Chiu, Y. K. Lo, and C. M. Leng, "LED backlight dirver circuit with dual-mode dimming control and current-balancing design," *IEEE Trans. Ind. Electron.*, Vol. 61, No. 9, pp. 4632-4639, Sep. 2014.

[14] Y. Qin, D. Lin, and S. Y. Hui, "A simple method for comparative study on the thermal performance of LEDs and Fluorescent lamps," *IEEE Trans. Power Electron.*, Vol. 24, No. 7, pp. 1811-1818, Jul. 2009.

[15] E. S. Lee, Y. H. Sohn, D. T. Nguyen, J. P. Cheon, and C. T. Rim, "LED driver with TRIAC dimming control by variable switched capacitance for power regulation," *Journal of Power Electronics*, Vol. 15, No. 2, pp. 555-566, Mar. 2015.

[16] H. L. Cheng and C. W. Lin, "Design and implementation of a high-power-factor LED driver with zero-voltage switching-on characteristics," *IEEE Trans. Power Electron.*, Vol. 29, No. 9, pp. 4949-4958, Sep. 2014.

[17] S. S. Hwang, W. S. Hwang, B. J. Jang, and S. K. Han, "Cost-effective single switch multi-channel LED driver," in *16th International Power Electronics and Motion Control Conference and Exposition (PEMC)*, pp. 156-161, Sep. 2014.

[18] Website of China Electric Mfg. corporation: http://www.toa.com.tw/

[19] Website of Everlight Electronics: http://www.everlight.com/

[20] J. M. Alonso, D. Gacio, A. J. Calleja, J. Ribas, and E. L. Corominas, "A study on LED retrofit solutions for low-voltage halogen cycle lamps," *IEEE Trans. Ind. Appl.*, Vol. 48, No. 5, pp. 1673–1682, Sep./Oct. 2012.

[21] N. Chen and H.S.-H. Chung, "A driving technology for retrofit LED lamp for fluorescent lighting fixtures with electronic ballasts," *IEEE Trans. Power Electron*, Vol. 26, No. 2, pp. 588-601, Feb. 2011.

[22] N. Chen and H.S.-H. Chung, "A universal driving technology for retrofit LED lamp for fluorescent lighting fixtures," in *27th Annual IEEE Applied Power Electronics Conference and Exposition (APEC)*, pp. 980-987, Feb. 2012.

[23] *19W, Single-stage AC/DC LED driver for T8/T10 fluorescent lamp replacement*, Texas Instruments, pp. 1-21, Apr. 2011.

[24] *User guide for FEBFL7701 L34U018A evaluation board universal input 18.3W LED driver*, Fairchild Semiconductor, pp. 1-24, Oct. 2012.

[25] *Low line only, high efficiency (>87%) high power factor (>0.98) low A-THD (<10%) 20W output non-isolated buck boost LED driver using LinkSwitch™-PL LINK460KG*, Power Integration, pp. 1-34, Sep. 2012.

[26] C. A. Cheng, C. H. Chang, H. L. Cheng, and T. Y. Chung, "A single-stage high-PF driver for supplying a T8-type LED lamp," in *International Power Electronics Conference (IPEC-Hiroshima 2014 – ECCE Asia)*, pp. 2523-2528, May 2014.

[27] M. K. Kazimierczuk and D. Czarkowski, *Resonant Power Converters*, New York: Wiley, 1995.

Chun-An Cheng was born in Kaohsiung, Taiwan, in 1974. He received his B.S. degree in Electrical Engineering from the National Taipei University of Technology, Taipei, Taiwan, in 1998, and his Ph.D. degree in Electrical Engineering from the National Cheng Kung University, Tainan, Taiwan, in 2006. Since August 2006, he has been with the Faculty of the Department of Electrical Engineering, I-Shou University, Kaohsiung, Taiwan, where he is currently an Associate Professor. In May 2011, he received the Excellent Electrical Engineer award from the Chinese Institute of Electrical Engineering (CIEE), Kaohsiung, Taiwan. His main research interests include power electronics, converters, inverters, and electronic ballasts/drivers for lighting applications. In addition, he holds three U.S. patents and eight Taiwan patents.

Chien-Hsuan Chang was born in Kaohsiung, Taiwan, in 1974. He received his B.S. degree in Electrical Engineering from the National Sun Yat-Sen University, Kaohsiung, Taiwan, in 1996, and his M.S. and Ph.D. degrees in Electrical Engineering from the National Chung Cheng University, Chiayi, Taiwan, in 1998 and 2002, respectively. From 2002 to 2007, he was a Chief Engineer and Team Leader with the Department of Telecom Power Module, Acbel Polytech Inc., Tamsui, Taipei, Taiwan, where he designed and developed high-power density and high-efficiency power modules for telecom applications. Since February 2007, he has been with the Department of Electrical Engineering, I-Shou University, Kaohsiung, Taiwan, where he is currently an Associate Professor. His current research interests include power electronic converters and their applications in photovoltaic power systems and LED drivers.

Hung-Liang Cheng was born in Chunghwa, Taiwan, in 1964. He received his B.S., M.S., and Ph.D. degrees in Electrical Engineering from the National Sun Yat-Sen University, Kaohsiung, Taiwan, in 1986, 1988, and 2001, respectively. From 1988 to 2007, he was an Electronic Researcher with the Chung-Shan Institute of Science and Technology, Taoyuan County, Taiwan, where he designed and developed high-power transmitters in radar and missile systems. Since February 2007, he has been with the Department of Electrical Engineering, I-Shou University, Kaohsiung, Taiwan, where he is currently a Professor. His current research interests include power electronic converters and electronic ballasts/drivers for lighting applications.

Tsung-Yuan Chung was born in Pingtung, Taiwan, in 1989. He received his M.S. degree in Electrical Engineering from I-Shou University, Kaohsiung, Taiwan, in 2014. Since November 2014, he has been with the Ablerex Electronics Co., Ltd., Kaohsiung, Taiwan, where he is currently a Hardware Engineer. His research interests include power electronic converters and LED drivers.

Ching-Shien Tseng was born in Tainan, Taiwan, in 1990. He received his M.S. degree in Electrical Engineering from I-Shou University, Kaohsiung, Taiwan, in 2015. Since October 2015, he has been with the National Chung-Shan Institute of Science &Technology, Taiwan, where he is currently an Associate Engineer. His research interests include power converters and electronic ballasts for lighting applications.

Kuo-Ching Tseng was born in Tainan, Taiwan, R.O.C., in 1957. He received his M.S. degree in Electrical Engineering from Da-Yeh Polytechnic Institute, Chang Hua, Taiwan, in 1999. From July 1988 to 1996, he was an R&D Engineer with Lumen Co., Ltd., Taiwan, R.O.C., where he worked on uninterruptible power supplies (UPSs) and switching power supply design. He received his Ph.D. degree in Electrical Engineering from National Cheng Kung University, Tainan, Taiwan, in 2004. In February 2003, he joined the Department of Electrical Engineering, Da-Yeh Institute of Technology. Since 2008, he has been with the Department of Electronic Engineering, National Kaohsiung First University of Science and Technology, Kaohsiung, Taiwan, where he is currently an Associate Professor. He received the Electric Power Applications Premium for his paper entitled "Novel High-Efficiency Step-Up Converter" from the Institution of Electrical Engineers (IEE) in 2004/2005. His current research interests include DC/DC converters and power factor correction techniques, power management control system design, solar energy conversion system design, switching power converter design, renewable energy conversion system design, and hydrogen energy and fuel cell power conversion systems. In addition, he holds seven Taiwan patents.